NIH Public Access
Author Manuscript
Mol Cell Neurosci. Author manuscript; available in PMC 2009 September 1.

Published in final edited form as:
Mol Cell Neurosci. 2008 September ; 39(1): 74–82. doi:10.1016/j.mcn.2008.05.017.

Multiple Cell Adhesion Molecules Shaping a Complex Nicotinic Synapse on Neurons

Gallen B. Triana-Baltzer, **Zhaoping Liu**[1], **Natalia V. Gounko**, and **Darwin K. Berg**[*]
Neurobiology Section, Division of Biological Sciences, University of California, San Diego, La Jolla, CA 92093-0357

Abstract

Neuroligin, SynCAM, and L1-CAM are cell adhesion molecules with synaptogenic roles in glutamatergic pathways. We show here that SynCAM is expressed in the chick ciliary ganglion, embedded in a nicotinic pathway, and, as shown previously for neuroligin and L1-CAM, acts transcellularly to promote synaptic maturation on the neurons in culture. Moreover, we show that electroporation of chick embryos with dominant negative constructs disrupting any of the three molecules in vivo reduces the total amount of presynaptic SV2 overlaying the neurons expressing the constructs. Only disruption of L1-CAM and neuroligin, however, reduces the number of SV2 puncta specifically overlaying nicotinic receptor clusters. Disrupting L1-CAM and neuroligin together produces no additional decrement, indicating that they act on the same subset of synapses. SynCAM may affect synaptic maturation rather than synapse formation. The results indicate that individual neurons can express multiple synaptogenic molecules with different effects on the same class of nicotinic synapses.

Keywords

nicotinic; neuroligin; SynCAM; L1; ciliary; synapse

Introduction

Single-pass transmembrane cell adhesion molecules (CAMs) are increasingly being implicated in synaptic maturation and function (Akins and Biederer, 2006; Craig and Kang, 2007). Two CAMs for which the evidence is most abundant are neuroligin (NL) and synaptic cell adhesion molecule (SynCAM). Postsynaptic NL participates in transcellular interactions with β-neurexin in the presynaptic terminal to align pre- and postsynaptic elements at glutamatergic synapses (Ichtchenko et al., 1995; Scheiffele et al., 2000; Dean et al., 2003; Boucard et al., 2005). Similarly, SynCAM participates in transcellular interactions with other SynCAMs to align pre- and postsynaptic components at glutamatergic synapses (Biederer et al., 2002; Biederer, 2005; Fogel et al., 2007). A third CAM, L1, has also been implicated in synaptic function (Luthl et al., 1994; Scholey et al., 1995; Law et al., 2003; Matsumoto-Miyai et al., 2003; Saghatelyan et al., 2004; Godenschwege et al., 2006).

[*]**Corresponding Author:** Darwin K. Berg, Neurobiology Section, Division of Biological Sciences; 0357; University of California, San Diego; 9500 Gilman Drive; La Jolla, CA 92093-0357. Phone: 858-534-4680; Fax 858-534-7309; Email: dberg@ucsd.edu.
[1]**Current Address:** J. David Gladstone Institutes, 1650 Owens Street, San Francisco, CA 94158.

Publisher's Disclaimer: This is a PDF file of an unedited manuscript that has been accepted for publication. As a service to our customers we are providing this early version of the manuscript. The manuscript will undergo copyediting, typesetting, and review of the resulting proof before it is published in its final citable form. Please note that during the production process errors may be discovered which could affect the content, and all legal disclaimers that apply to the journal pertain.

NIH-PA Author Manuscript
NIH-PA Author Manuscript
NIH-PA Author Manuscript

NIH-PA Author Manuscript

NIH-PA Author Manuscript

NIH-PA Author Manuscript

Whether the three CAMs provide largely similar effects or have distinctive roles in synaptogenesis remains unclear. Both NL and SynCAM, when expressed in non-neuronal cells, can induce presynaptic specializations in adjacent neurons, but the two CAMs appear to have different effects when overexpressed in neurons themselves (Sara et al., 2005). Further, NL subtypes can contribute to GABAergic synapse formation, depending on the postsynaptic components available (Graf et al., 2004; Prange et al., 2004; Chih et al., 2005; Levinson et al., 2005; Gerrow et al., 2006; Kang et al., 2008); this has not been reported for the other CAMs. Also unresolved is the extent to which the CAMs direct the initial events of synapse formation in vivo versus acting to stabilize them or enhance function (Varoqueaux et al., 2006).

Recent studies indicate that NL and L1 are present in nicotinic pathways. Both NL and L1 are expressed in cholinergic neurons and contribute to nicotinic synapse formation in culture, and L1 has additionally been shown to promote innervation of muscle in vivo (Triana-Baltzer et al., 2006; Conroy et al., 2007). SynCAM has not been identified in nicotinic pathways.

An attractive system for comparing the roles of synaptogenic CAMs at nicotinic synapses is provided by the chick ciliary ganglion (CG) because the choroid and ciliary cells, which comprise almost all of CG neurons, receive nicotinic cholinergic input as their main form of chemical transmission (Dryer, 1994). CG neurons express two principal classes of nicotinic acetylcholine receptors (nAChRs): homopentameric receptors containing α7 subunits (α7-nAChRs) that are clustered on somatic spines (Shoop et al., 1999, 2002), and heteropentameric receptors containing α3 subunits (α3*-nAChRs) concentrated at postsynaptic densities (Conroy and Berg, 1995; Williams et al., 1998). Nicotinic transmission is mediated by a large preganglionic calyx engulfing each ciliary neuron and by numerous synaptic boutons contacting each choroid neuron.

Here we show that CG neurons express SynCAM and that it co-localizes with α7-nAChR clusters on the neurons. Moreover, as found previously for NL and L1, SynCAM can act transcellularly to induce presynaptic specializations in adjacent cholinergic neurons in culture. We show here that all three can do so in vivo. The three differ, however, in their ability to promote alignment of pre- and postsynaptic components, suggesting different roles during synaptogenesis.

Results

SynCAM Expression in the Chick CG

Nicotinic synapses are consolidated on chick CG neurons between embryonic day (E) 7 and E14 (Landmesser and Pilar, 1974). Western blots of E14 CG extracts probed with an anti-SynCAM polyclonal antibody (Fig. 1A) showed bands corresponding to core and heavily glycosylated SynCAM (Biederer et al., 2002). Immunostaining freshly dissociated E14 CGs with the anti-SynCAM antibody revealed large clusters that co-distributed with Alexa488-α-bungarotoxin (AlexaBgt) staining, a specific probe for α7-nAChRs (Fig. 1B–D). The SynCAM clusters also co-distributed in part with L1, previously found to localize with both α7-nAChRs and α3*-nAChRs (Triana-Baltzer et al., 2006), but SynCAM did not co-localize with α3*-nAChRs when they were imaged (not shown). The SynCAM immunostaining was specific: it could not be mimicked by substituting non-immune Ig for the primary antibody (Fig. 1E), and it was blocked by preabsorbing the primary antibody with a peptide corresponding to the SynCAM cytoplasmic domain used as immunogen to raise the antibody originally (Fig. 1F–H). Because the antibody does not distinguish between SynCAM 1 and 2 (Fogel et al., 2007), we use SynCAM here to signify either or both. The results show that SynCAM is expressed by CG neurons and co-localizes with α7-nAChRs and in part with L1 on the cells.

NIH-PA Author Manuscript

NIH-PA Author Manuscript

NIH-PA Author Manuscript

SynCAM can act transcellularly to induce presynaptic specializations in cholinergic neurons. This was shown by expressing a SynCAM construct tagged with green fluorescent protein (Syn-GFP) in HEK293 cells and combining the cells with CG neurons in culture. Immunostaining after several days for SV2 protein as a presynaptic marker showed that most of the transfected HEK cells were contacted by neurites displaying multiple SV2 clusters immediately adjacent to the HEK cell body (Fig. 2A). In contrast, HEK cells transfected with a GFP construct as a negative control rarely were juxtaposed to SV2 clusters (Fig. 2B). The results were quantified by scoring the proportion of HEK cells receiving at least two SV2 clusters (Fig. 2C). By this criterion SynCAM significantly increased the ability of transfected HEK cells to accumulate presynaptic specializations from passing CG neurites. Similar results were previously obtained with NL and L1 in this assay (Triana-Baltzer et al., 2006;Conroy et al., 2007).

Dominant Negative Analysis of CAM Actions in Ovo

Finding that three putative synaptogenic CAMs are expressed in CG neurons at a time when nicotinic synapses are maturing on the cells raised questions about their possibly unique contributions. This was examined by electroporating dominant negative constructs of the three CAMs separately into CG precursors in ovo and evaluating the developmental consequences as previously described (Liu et al., 2006). The constructs encoded fusion proteins containing either the entire cytoplasmic domains of SynCAM or L1, or the 54 amino acids in the membrane-proximal region of the cytoplasmic domain of NL – all tagged with GFP for ready visualization (SynCyt-GFP, L1Cyt-GFP, and NL54-GFP, respectively). These cytoplasmic fragments have previously been shown to act as dominant negatives in cell culture (Biederer et al., 2002; Triana- Baltzer et al., 2006; Conroy et al., 2007). The NL dominant negative construct is likely to target all three NL subtypes expressed in the CG (Ross and Conroy, 2008). Here and below, NL is used to refer collectively to the family of NL subtypes (NL-1, -3, and -4) expressed in the ganglion. Similarly, the SynCAM dominant negative is likely to target all SynCAM isoforms.

Chick embryos were electroporated at E2, returned to the incubator, and taken for analysis at E14, a time when both choroid and ciliary neurons have relatively mature nicotinic synapses (Landmesser and Pilar, 1974). The CG was dissected, immunostained for the presynaptic marker SV2 and the postsynaptic receptor α3*-nAChR, sectioned, and imaged. Individual electroporated neurons expressing the construct were readily apparent within the population of ganglionic neurons and could be assessed for receptor clusters and proximal SV2 staining (Fig. 3).

Quantifying the amount of immunostaining in such experiments showed that L1Cyt-GFP, NL54-GFP, and SynCyt-GFP each caused the electroporated neuron to receive significantly less SV2 immunostaining overlaying the soma than found on nearby unelectroporated neurons (Fig. 4A). GFP, used as a negative control, had no effect on SV2 levels. Quantifying the number of SV2 puncta and the mean size of puncta overlaying the soma indicated that NL54-GFP nominally produced the greatest deficit in the former while L1Cyt and SynCyt significantly reduced the latter (Fig. 4B,C). None changed the mean intensity of SV2 puncta contacting the soma (Fig. 4D). None of the constructs visibly altered any of these four parameters for α3*-nAChRs on the neurons, i.e. no change in the amount of cell surface containing α3*-nAChRs (Fig. 4E) and no change in the number, size, or mean intensity of staining for α3*-nAChR clusters (Fig. 4F–H).

While increases in presynaptic markers such as SV2 can be viewed as a synaptogenic effect, a more stringent criterion for synapse formation is the alignment of such presynaptic markers over postsynaptic receptor clusters. To evaluate this, we quantified the number and proportion of α3*-nAChR clusters with juxtaposed SV2 puncta. The L1 and NL dominant negative

NIH-PA Author Manuscript

NIH-PA Author Manuscript

NIH-PA Author Manuscript

constructs each induced a significant reduction in number of synaptic contacts measured either as the total number of α3*-nAChR clusters overlaid by SV2 puncta (Fig. 5A) or as the proportion of such clusters receiving SV2 puncta (Fig. 5B). The SynCAM dominant negative construct did not have a significant effect on either measure.

The absence of a SynCAM effect on SV2/α3*-nAChR alignment raised the question of whether it might instead influence this parameter for α7-nAChR clusters since SynCAM is preferentially colocalized with α7-nAChRs on the neurons. Though α7-nAChRs are not found in postsynaptic densities, they are activated by "ectopic" transmitter release and are overlaid by a diffuse distribution of SV2 puncta in vivo (Wilson Horch et al, 1995; Shoop et al., 1999; Coggan et al., 2005). Quantifying the effects of the SynCAM dominant negative, however, failed to detect a change in either the total number or the proportion of α7-nAChR clusters overlaid by SV2 puncta (Fig. 5C). L1Cyt-GFP, assayed for comparison, also had no effect on these parameters though it did reduce both for α3*-nAChR clusters as shown above. None of the constructs altered the amount of cell surface α7-nAChRs or the number, size, or mean intensity of staining for α7-nAChR clusters on the neurons (data not shown).

Use of RNAi to Manipulate CAM Actions in Ovo

The results with dominant negatives suggested that NL and L1 might both have synaptogenic roles, i.e. determine the number of synaptic contacts formed or stabilized, while SynCAM might act to promote synaptic maturation, i.e. increase the size of the contact. The synaptogenic effects of NL and L1 were further tested with specific RNAi constructs. Short hairpin RNA fragments (shRNA) directed against chicken NL or L1 were expressed in vectors encoding either GFP or red fluorescent protein (RFP) under separate promoters to confirm expression. The NL RNAi construct (RNAi-NL) was previously shown to be effective in cell culture (Conroy et al., 2007). Transfection of CG neurons in cell culture with the L1 RNAi construct (RNAi-L1) showed that it produced a strong reduction of endogenous L1 levels compared to those found in nearby untransfected cells (Fig. 6A). An RNAi with the same composition but scrambled sequence (RNAi-control) had no effect on L1 levels (Fig. 6B). Electroporating E2 chick embryos with RNAi-L1, followed by immunostaining for SV2 and α3*-nAChRs at E14, revealed a pattern similar to that seen previously with the dominant negative L1Cyt-GFP. RNAi-L1 significantly reduced the levels of SV2 staining overlaying the electroporated neuron and the proportion of synaptic α3*-nAChR clusters (Fig. 6C,D). No change was seen in the amount or distribution of α3*-nAChR revealed by immunostaining (not shown).

Electroporation of the RNAi-control produced no changes in either SV2 or α3*-nAChR staining patterns and levels, confirming specificity. Notably, the RNAi-NL construct had no effect on SV2 or synaptic staining patterns, unlike the dominant negative NL54-GFP construct (Fig. 6C,D). The ineffectiveness of the RNAi-NL construct presumably reflects the fact that it targets NL-1 uniquely, but CG neurons also express NL-3 and NL-4 (Ross and Conroy, 2008). Both the RNAi results and the dominant negative experiments demonstrate that L1 promotes the formation/stabilization of synaptic contacts on CG neurons in vivo.

Convergent CAM Effects on Nicotinic Synaptogenesis

The dominant negative analysis indicated that both L1 and NL are necessary to form or sustain nicotinic synapses on CG neurons. Whether they target the same or different synaptic populations was addressed by employing a double construct encoding both L1Cyt-GFP and NL54-GFP under separate promoters (L1Cyt/NL54). To confirm expression of both dominant negatives in the construct, we transfected CG neurons in culture with L1Cyt/NL54 and examined the outcome both by immunocytochemistry and by Western blot analysis. Since the L1 segment was from human L1, a human-specific anti-L1 antibody directed against the cytoplasmic domain was employed to visualize specific expression of L1Cyt, distinct from

NIH-PA Author Manuscript

NIH-PA Author Manuscript

NIH-PA Author Manuscript

endogenous chicken L1. Immunostaining for L1Cyt revealed strong expression in all L1Cyt-GFP-transfected neurons and not in untransfected neurons (Fig. 7A–D). Western blot analysis of cell lysates probed with an anti-GFP antibody revealed two distinct bands corresponding to the molecular weights of L1Cyt-GFP and NL54-GFP respectively (Fig. 7E). The results indicate that both dominant negatives are expressed when the construct is introduced into neurons.

Electroporation with L1Cyt/NL54, followed by immunostaining for SV2 and α3*-nAChRs as above, revealed synaptic structure perturbations comparable to that seen with L1Cyt-GFP or NL54-GFP alone. Thus, simultaneous expression of L1 and NL dominant negatives in the same postsynaptic neuron significantly reduced the levels of SV2 staining while not changing the amount or pattern of nAChR staining (data not shown). Calculating the proportion of α3*-nAChR clusters with associated SV2 staining also showed a reduction comparable to that obtained with either L1Cyt-GFP or NL54-GFP alone (Fig. 7F). The results indicate that L1 and NL are required for the same population of synapses.

Discussion

The results demonstrate that a population of cholinoceptive neurons may express up to three distinct CAMs capable of influencing the formation and/or stabilization of nicotinic synapses. Further, the CAMs all appear during the same developmental window when innervation is being consolidated on the neurons. The results show that each of the CAMs – L1, NL, and SynCAM – act in vivo to enhance the ability of preganglionic terminals to form synaptic specializations on the neurons. The CAMs do not, however, appear to be redundant. Judging from the incidence of SV2-containing puncta in presynaptic terminals aligning over α3*-nAChR clusters on the postsynaptic neuron, both L1 and NL are essential for optimal innervation. SynCAM appears to play a different role, affecting SV2-puncta size and possibly number but not the ability to align over postsynaptic receptors. The picture that emerges is one of collaboration in which several CAMs combine to determine the size and number of nicotinic synapses converging on a neuron.

L1 disruption with a dominant negative construct or knockdown with RNAi produced an overall reduction in the amount of presynaptic material judging by SV2 staining, and a loss in the number of SV2 puncta specifically aligned over α3*-nAChR clusters on the postsynaptic neuron. These findings suggest a specific role for L1 in the formation and/or stabilization of nicotinic synapses on neurons, acting from the postsynaptic side. Neurofascin, a member of the same CAM subfamily containing L1, has also been shown to promote the subcellular localization of presynaptic input in the cerebellum (Ango et al., 2004). In contrast to neurofascin and other putative synaptogenic CAMS including SynCAM, NL, EphB2, SALM, and NGL2, L1 does not contain a PDZ-binding domain to aid in protein interactions and scaffold localization (Biederer et al., 2002; Scheiffele et al., 2000; Kayser et al., 2006; Ko et al., 2006; Kim et al., 2006). How L1 exerts its effects on developing synapses is unknown.

The dominant negative approach indicated that also NL is required for full innervation of CG neurons in vivo, affecting the total amount of SV2 staining, the number of SV2 puncta abutting the cells, and the proportion of such puncta aligned over α3*-nAChR clusters. NL knockdown with an RNAi, however, had no effect. Most likely the RNAi was ineffective because it would have targeted only one of the three NL isoforms (NL1, 3, and 4) now known to be expressed in the CG (Ross and Conroy, 2008). Consistent with this view, significant effects on mouse respiratory function and viability are not apparent until multiple NL genes are deleted (Varoqueaux et al., 2006). NL54-GFP does reduce the frequency of miniature excitatory postsynaptic potentials in CG neurons in culture, indicating its competence (Conroy et al., 2007). The construct likely interferes with NL 1, 3, and 4 because of the high degree of

NIH-PA Author Manuscript

NIH-PA Author Manuscript

NIH-PA Author Manuscript

conservation among them (66% similarity at the amino acid level among chicken NL1-NL3; 81% with mouse/rat NL1-NL4). The fact that NL54-GFP, which lacks a PDZ-binding domain, is able to disrupt synaptic development in vivo suggests that the membrane-proximal portion of NL is likely to contain relevant domains.

SynCAM, the third synaptogenic candidate examined, has not previously been implicated in nicotinic pathways. We show here that SynCAM is expressed by cholinergic neurons, localizes with α7-nAChRs on the cells, and has the capacity to organize presynaptic components on adjacent cholinergic processes in cell culture. In vivo, however, SynCAM does not appear to be essential at least for initiation of nicotinic synaptic contacts. The number of SV2 puncta overlaying either α3*-nAChR or α7-nAChR clusters was not significantly reduced by the SynCAM dominant negative. While it is possible that multiple SynCAM family members are expressed in CG neurons, the dominant negative construct used here should have disrupted all of them. The construct encodes the entire cytoplasmic domain of mouse SynCAM1, and chicken and mouse SynCAM1 cytoplasmic domains are 100% identical at the amino acid level. The dominant negative used here did reduce the total amount of SV2 staining in preganglionic terminals contacting the neurons, indicating that it was effective. A similar dominant negative construct encoding the cytoplasmic domain of mouse SynCAM is able to disrupt the number and size of presynaptic puncta in hippocampal cultures (Biederer et al., 2002). The results obtained here suggest that SynCAM may play a role in stabilizing or promoting the maturation of nicotinic synapses, but that it is not necessary for nicotinic synapse formation de novo.

NL on CG neurons is very likely to interact with β-neurexin on preganglionic terminals while L1 may interact either with presynaptic L1 or another component (Triana-Baltzer et al., 2006; Conroy et al., 2007; Ross and Conroy, 2008). SynCAM can participate in homophilic interactions with other members of the SynCAM family (Biederer et al., 2002, Fogel et al., 2007) and may recognize such components on the preganglionic terminal. Both NL and L1 are required for full innervation in vivo, and appear to act on the same subset of synapses because a double NL/L1 dominant negative did not reduce the incidence of synapses below that seen with either the NL or L1 dominant negatives alone. Though L1 is localized at both α3*-nAChR and α7-nAChR clusters, it helps align SV2 puncta over only a portion of the α3*-nAChRs. A substantial population of synapses on CG neurons, involving both α3*-nAChR and α7-nAChR clusters, apparently require neither NL nor L1 for initiation. SynCAM also appears to be dispensable for this task since the SynCAM dominant negative was unable to reduce the number of SV2 puncta aligned over α3*-nAChR clusters or over α7-nAChR clusters where SynCAM is most prominent. The results indicate that NL, L1, and SynCAM play different roles in shaping nicotinic synapses on neurons and that other yet to be identified synaptogenic molecules are likely to contribute as well. One such candidate may be the EphB2 receptor (Dalva et al., 2007) which has recently been shown to co-distribute with α7-nAChRs on CG neurons and to influence their stability and down-stream signaling (Liu et al., 2008).

Experimental Methods

CG cultures

Dissociated embryonic day (E) 8 CG neurons were maintained in cell culture for 7–10 days on glass coverslips coated with poly-D-lysine, fibronectin, and lysed fibroblasts (Nishi and Berg, 1981; Zhang et al., 1994). Dissociated E14 CG neurons were maintained for 1–4 hours on glass coverslips coated as above except lacking fibroblasts (Conroy et al., 2003). Co-cultures of E8 CG neurons and HEK293 cells were prepared by transfecting HEK293 cells and adding them to CG cultures prepared 4 days earlier. The co-cultures were taken for analysis after an additional 48–56 hours before fixation (Triana-Baltzer et al., 2006).

NIH-PA Author Manuscript

NIH-PA Author Manuscript

NIH-PA Author Manuscript

Transfections

Transient transfections were performed on HEK293 by calcium phosphate precipitation (Conroy and Berg, 1998). E8 CG neurons in culture were transfected with RNAi constructs at the time of plating as previously described (Conroy et al., 2003) using the transfection reagent Effectene (Qiagen, 0.25–0.5 μg DNA/well, 1:25 ratio DNA:Effectene). After 24 hours the medium was replaced with fresh medium. Cultures were analyzed after 7–10 days. Typical transfection efficiencies were 1–2%. CG neuron precursors were transfected in vivo by electroporation.

The SynCAM constructs used here encode all or parts of the mouse SynCAM 1 sequence (full length construct kindly provided by Dr. Thomas Biederer, Yale University). SynCAM-GFP encodes the entire SynCAM protein with a GFP tag fused at the C-terminus, while SynCyt-GFP encodes only the cytoplasmic domain of SynCAM with a GFP tag fused at the N-terminus. The L1 construct used here encodes part of the human L1 sequence (full length construct kindly provided by Dr. Anthony Montgomery, UCSD). L1Cyt-GFP encodes only the cytoplasmic domain of L1 with a GFP tag fused at the N-terminus. The NL construct used here encodes part of the rat NL-1 sequence (construct kindly provided by Dr. William G. Conroy, UCSD). NL54-GFP encodes 54 membrane-proximal amino acids of the cytoplasmic domain of NL with a GFP tag fused at the N-terminus (Conroy et al., 2007). All full-length or truncated constructs were prepared by subcloning the appropriate sequences into mammalian expression vectors providing either a C- or N-terminal GFP tag (pEGFPN1 or C1 vectors respectively, Clontech, Palo Alto, CA). The L1Cyt/NL54 construct was generated by subcloning the entire L1Cyt-GFP cassette, including the intact pCMV promoter and SV40 polyA signal, upstream of the similar NL54-GFP cassette.

RNA interference

RNAi-L1 was constructed by targeting two spots in the chicken L1 (NgCAM) sequence GCGACATCGTTCACATCGCTCA and GACTACATCTGCCACGCTCACT with the intention of suppressing L1 expression. A control short hairpin RNA was constructed using the scrambled sequence AGTTCGAAGTCCAATTCATGAA. Both of these cassettes were subcloned into the expression vector pRFPRNAiC (ARK-Genomics, Roslin Institute, Roslin, U.K.) that uses a chick U6 promoter to drive expression of an RNA cassette with chick-specific microRNA flanking sequences (with specific RNAi target sequence inserted within) and carries an RFP tag under control of a β-actin promoter to track transfection. The RNAiNL construct targets chicken NL 1 and has been characterized previously (Conroy et al., 2007) (construct kindly provided by William G. Conroy, UCSD).

In ovo electroporation

DNA constructs were injected into the lumen of stage 7–9 chick embryonic spinal cords (Hamburger and Hamilton, 1951). Precise staging of the embryos was critical and was usually obtained from eggs incubated for 38–41 hours at 37°C. Electroporation was performed using a square wave electroporator (BTX, San Diego, CA) with five 50 millisecond pulses of 25 mV current at 1 Hz. as previously described (Triana-Baltzer et al., 2006). Embryos were harvested 12 days later (E14), and both ciliary ganglia were dissected, stained, and fixed in 4% (wt/vol) paraformaldehyde (PFA) in 0.1 M sodium phosphate (pH 7.4) for 1 hour at room temperature.

Fluorescence Microscopy

For dissociated E14 CG neurons surface α7-nAChRs were labeled by adding Alexa488-αBungarotoxin (Alexa488-αBgt; 100 nM; Molecular Probes, Eugene, OR) to the cell media for 20 minutes at 37°C. After rinsing in Gey's Balanced Salt Solution, the cells were fixed with 2% PFA for 20 minutes at room temperature. For HEK/CG cocultures cells were rinsed in

NIH-PA Author Manuscript

NIH-PA Author Manuscript

NIH-PA Author Manuscript

room temperature PBS (150 mM NaCl, 10 mM sodium phosphate, pH 7.4) followed by fixation as above.

For E14 electroporated CG surface α3*- or α7-nAChRs were labeled by immediately incubating dissected whole CG with the anti-α1/α3/α5 monoclonal antibody (mAb) (mAb35) (1:500; Conroy and Berg, 1998) or rhodamine-αBgt (1:1000), respectively for 1 hour at 4°C in PBS containing 5% normal donkey serum. After rinsing in PBS for 30 minutes at 4°C, the ganglia were fixed with 4% PFA for 1 hour at room temperature. After further rinsing in PBS for 30 minutes at 4°C, the ganglia were incubated in 30% sucrose for 2 hours at 4°C, embedded in Tissue-Tek O.C.T. compound (Sakuro Fineteck USA, Torrance, CA), frozen overnight at −20°C, and sectioned at 40 μm using a CM 1900 cryostat (Leica Microsystems, Nussloch, Germany). After rehydration in 0.1x PBS for 10 minutes, the sections were immunostained for presynaptic components.

To label intracellular antigens cells/sections were incubated with appropriate dilutions of rabbit anti-SynCAM polyclonal antibody (pAb) (1:1000; Novus Biologicals, Littleton, CO), non-immune rabbit Ig (Jackson Immunoresearch Laboratories, West Grove, PA), mouse anti-chick L1 mAb (1:20,, clone 8D9, Developmental Studies Hybridoma Bank, University of Iowa), goat anti-human L1 pAb (1:500, Santa Cruz Biotechnology Inc., Santa Cruz, CA), or anti-SV2 and/or anti-synaptotagmin mAbs (1:40; Developmental Studies Hybridoma Bank) overnight at 4°C in PBS containing 5% normal donkey serum and 0.05% Triton X-100. CG sections were colabeled with both anti-SV2 and anti-synaptotagmin in order to boost signal for presynaptic proteins as described previously (Gautam et al., 1996). After washing in PBS with 0.05% Triton X-100 (PBS-Tx) the cells/sections were incubated with appropriate donkey Cy3-, Cy5- or FITC-conjugated secondary antibodies (Jackson Immunoresearch Laboratories) for 1 hour at room temperature. After rinsing in PBS-Tx, the cells/sections were viewed with a 63x, 1.4 NA objective on a Zeiss Axiovert equipped with CCD camera and digital imaging with Slidebook software (Intelligent Imaging Innovations, Santa Monica, CA). For visualization, reconstructed images were generated from *z*-axis stacks of 0.5 μm deconvolved optical sections. Control and experimental images were taken with the same exposure settings and displayed with the same dynamic range of pixel intensities for direct comparison.

Quantification protocols

For HEK/CG cocultures the proportion of transfected HEK cells contacted by 2 or more SV2 puncta (boutons) was quantified as described previously (Triana-Baltzer et al., 2006). For CG sections, fields containing both a transfected and numerous untransfected ciliary neurons were randomly selected and imaged. Choroid neurons (small cells) were not used for quantification due to uncertainties about their cell borders and synaptic alignment. For quantification of relative receptor and SV2/synaptotagmin staining, 2–4 nearby untransfected cells of similar size and morphology were chosen for normalization from deconvolved images. Background staining was subtracted from the images. Cell surfaces were masked for analysis by highlighting the perimeter of the cell surface with a drawing tool having a width of 12 pixels (1.2 μm); thus the area within 1.2 μm of the cell surface was analyzed. Clusters within the masked area were defined as having at least 5 contiguous pixels with specific staining. Clusters of SV2 were counted manually as being aligned with nAChR clusters if they were within 4 pixels (0.4 μm) of each other. Statistical significance was assessed by Students' *t*-test or ANOVA with a Bonferroni post-test.

Immunoblots

Extracts were prepared from E14 chick CG, subjected to SDS-PAGE, transferred to nitrocellulose blots, and assayed as previously described (Conroy et al., 2003). Anti-SynCAM pAb was used at 1:1000; non-immune rabbit Ig was used at the same concentration. For analysis

NIH-PA Author Manuscript

NIH-PA Author Manuscript

NIH-PA Author Manuscript

of L1Cyt/NL54 expression transfected E8 CG cultures were scraped with SDS sample buffer, boiled at 95 °C for 5 minutes, and then subjected to Western blot procedures as above. Primary antibody used here was rabbit anti-GFP pAb (1:100, Clontech).

Materials

White leghorn chick embryos were obtained locally and maintained in a humidified incubator. All other reagents were purchased from Sigma unless otherwise indicated.

Acknowledgements

Grant support was provided by the National Institutes of Health Grants NS12601 and NS35469 and by the Tobacco-Related Disease Research Program 16RT-0167. We thank Xiao-Yun Wang for expert technical assistance.

References

Akins MR, Biederer T. Cell-cell interactions in synaptogenesis. Curr. Op. Neurobiol 2006;16:83–89. [PubMed: 16427268]

Ango F, di Cristo G, Higashiyama H, Bennett V, Wu P, Huang ZJ. Ankyrin-based subcellular gradient of neurofascin, an immunoglobulin family protein, directs GABAergic innervation at Purkinje axon initial segment. Cell 2004;119:257–272. [PubMed: 15479642]

Biederer T, Sara Y, Mozhayeva M, Atasoy D, Liu X, Kavalali EG, Sudhof TC. SynCAM, a synaptic adhesion molecule that drives synapse assembly. Science 2002;297:1525–1531. [PubMed: 12202822]

Biederer T. Bioinformatic characterization of the SynCAM family of immunoglobulin-like domain-containing adhesion molecules. Genomics 2005;87:139–150. [PubMed: 16311015]

Boucard AA, Chubykin AA, Comoletti D, Taylor P, Sudhof TC. A splice code for trans-synaptic cell adhesion mediated by binding of neuroligin-1 to α- and β-neurexins. Neuron 2005;48:229–236. [PubMed: 16242404]

Chih B, Engelman H, Scheiffele P. Control of excitatory and inhibitory synapses formation by neuroligins. Science 2005;307:1324–1328. [PubMed: 15681343]

Coggan JS, Bartol TM, Esquenazi E, Stiles JR, Lamont S, Martone ME, Berg DK, Ellisman MH, Sejnowski TJ. Ectopic neurotransmitter release at a neuronal synapse. Science 2005;309:446–451. [PubMed: 16020730]

Conroy WG, Berg DK. Neurons can maintain multiple classes of nicotinic acetylcholine receptors distinguished by different subunit compositions. J. Biol. Chem 1995;270:4424–4431. [PubMed: 7876208]

Conroy WG, Berg DK. Nicotinic receptor subtypes in the developing chick brain: appearance of a species containing the α4, β2, and α5 gene products. Mol. Pharmacol 1998;53:392–401. [PubMed: 9495803]

Conroy WG, Liu Z, Nai Q, Coggan J, Berg DK. PDZ-containing proteins provide a functional postsynaptic scaffold for nicotinic receptors in neurons. Neuron 2003;38:759–771. [PubMed: 12797960]

Conroy WG, Nai Q, Ross B, Naughton G, Berg DK. Postsynaptic neuroligin enhances presynaptic inputs at neuronal nicotinic synapses. Dev. Biol 2007;307:79–91. [PubMed: 17521624]

Craig AM, Kang Y. Neurexin-neuroligin signaling in synapse development. Curr. Op. Neurobiol 2007;17:43–52. [PubMed: 17275284]

Dalva MB, McClelland AC, Kayser MS. Cell adhesion molecules: signalling functions at the synapse. Nat. Rev. Neurosci 2007;8:206–220. [PubMed: 17299456]

Dean C, Scholl FG, Choih J, DeMaria S, Berger J, Isacoff E, Scheiffele P. Neurexin mediates the assembly of presynaptic terminals. Nat. Neurosci 2003;6:708–716. [PubMed: 12796785]

Dryer SE. Functional development of the parasympathetic neurons of the avian ciliary ganglion: a classic model system for the study of neuronal differentiation and development. Prog. Neurobiol 1994;43:281–332. [PubMed: 7816929]

Fogel AI, Akins MR, Krupp AJ, Stagi M, Stein V, Biederer T. SynCAMs organize synapses through heterophilic adhesion. J. Neurosci 2007;27:12516–12530. [PubMed: 18003830]

NIH-PA Author Manuscript

NIH-PA Author Manuscript

NIH-PA Author Manuscript

Gautam M, Noakes PG, Moscoso L, Rupp F, Scheller RH, Merlie JP, Sanes JR. Defective neuromuscular synaptogenesis in agrin-deficient mutant mice. Cell 1996;85:525–535. [PubMed: 8653788]

Gerrow K, Romorini S, Nabi SM, Colicos MA, Sala C, El-Husseini A. A preformed complex of postsynaptic proteins is involved in excitatory synapse development. Neuron 2006;49:547–562. [PubMed: 16476664]

Godenschwege TA, Kristiansen LV, Uthaman SB, Hortsch M, Murphey RK. A conserved role for drosophila neuroglian and human L1-CAM in central-synapse formation. Curr. Biol 2006;16:12–23. [PubMed: 16401420]

Graf ER, Zhang XZ, Jin S-X, Linhoff MW, Craig A-M. Neurexins induce differentiation of GABA and glutamate postsynaptic specializations via neuroligins. Cell 2004;119:1013–1026. [PubMed: 15620359]

Hamburger V, Hamilton H. A series of normal stages in the development of chick embryo. J. Morphol 1951;88(8):49–92.

Ichtchenko K, Hata Y, Nguyen T, Ullrich B, Missler M, Moomaw C, Sudhof TC. Neuroligin 1: a splice site-specific ligand for β-neurexins. Cell 1995;81:435–443. [PubMed: 7736595]

Kang Y, Zhang XZ, Bobie F, Wu H, Craig AM. Induction of GABAergic postsynaptic differentiation by α-neurexins. J. Biol. Chem 2008;283:2323–2334. [PubMed: 18006501]

Kayser MS, McClelland AC, Hughes EG, Dalva MB. Intracellular and trans-synaptic regulation of glutamatergic synaptogenesis by EphB receptors. J. Neurosci 2006;26:12152–12164. [PubMed: 17122040]

Kim S, Burette A, Chung HS, Kwon SK, Woo J, Lee HW, Kim K, Kim H, Weinberg RJ, Kim E. NGL family PSD-95-interacting adhesion molecules regulate excitatory synapse formation. Nat. Neurosci 2006;9:1203–1204. [PubMed: 17001334]

Ko J, Kim S, Chung HS, Kim K, Han K, Kim H, Jun H, Kaang BK, Kim E. SALM synaptic cell adhesion-like molecules regulate the differentiation of excitatory synapses. Neuron 2006;50:233–245. [PubMed: 16630835]

Landmesser L, Pilar G. Synapse formation during embryogenesis on ganglion cells lacking a periphery. J. Physiol 1974;241:715–736. [PubMed: 4373567]

Law JW, Lee AY, Sun M, Nikonenko AG, Chung SK, Dityatev A, Schachner M, Morellini F. Decreased anxiety, altered place learning, and increased CA1 basal excitatory synaptic transmission in mice with conditional ablation of the neural cell adhesion molecule L1. J. Neurosci 2003;23:10419–10432. [PubMed: 14614101]

Levinson JN, Chery N, Huang K, Wong TP, Gerrow K, Kang R, Prange O, Wang YT, El-Husseini A. Neuroligins mediate excitatory and inhibitory synapse formation. Involvement of PSD-95 and neurexin-1β in neuroligin-induced synaptic specificity. J. Biol. Chem 2005;280:17312–17319. [PubMed: 15723836]

Liu Z, Conroy WG, Stawicki TM, Nai Q, Neff RA, Berg DK. EphB receptors co-distribute with a nicotinic receptor subtype and regulate nicotinic downstream signaling in neurons. Molec. Cell. Neurosci. 2008in press.

Liu Z, Neff RA, Berg DK. Sequential interplay of nicotinic and GABAergic signaling guides neuronal development. Science 2006;314:1610–1613. [PubMed: 17158331]

Luthl A, Laurent JP, Figurov A, Muller D, Schachner M. Hippocampal long-term potentiation and neural cell adhesion molecules L1 and NCAM. Nature 1994;372:777–779. [PubMed: 7997264]

Matsumoto-Miyai K, Ninomiya A, Yamasaki H, Tamura H, Nakamura Y, Shiosaka S. NMDA-dependent proteolysis of presynaptic adhesion molecule L1 in the hippocampus by neuropsin. J. Neurosci 2003;23:7727–7736. [PubMed: 12944500]

Nishi R, Berg DK. Two components from eye tissue that differentially stimulate the growth and development of ciliary ganglion neurons in cell culture. J. Neurosci 1981;1:505–513. [PubMed: 7346565]

Prange O, Wong TP, Gerrow K, Wang YT, El-Husseini A. A balance between excitatory and inhibitory synapses is controlled by PSD-95 and neuroligin. Proc. Natl. Acad. Sci. (USA) 2004;101:13915–13920. [PubMed: 15358863]

Ross BS, Conroy WG. Capabilities of neurexins in the chick ciliary ganglion. Dev. Neurobiol 2008;68:409–419. [PubMed: 18161851]

NIH-PA Author Manuscript

NIH-PA Author Manuscript

NIH-PA Author Manuscript

Saghatelyan AK, Nikonenko AG, Sun M, Rolf B, Putthoff P, Kutsche M, Bartsch U, Dityatev A, Schachner M. Reduced GABAergic transmission and number of hippocampal perisomatic inhibitory synapses in juvenile mice deficient in the neural cell adhesion molecule L1. Mol. Cell. Neurosci 2004;26:191–203. [PubMed: 15121190]

Sara Y, Biederer T, Atasoy D, Chubykin A, Mozhayeva MG, Sudhof TC, Kavalali ET. Selective capability of SynCAM and neuroligin for functional synapse assembly. J. Neurosci 2005;25:260–270. [PubMed: 15634790]

Scheiffele P, Fan J, Choih J, Fetter R, Serafini T. Neuroligin expressed in nonneuronal cells triggers presynaptic development in contacting axons. Cell 2000;101:657–669. [PubMed: 10892652]

Scholey AB, Mileusnic R, Schachner M, Rose SP. A role for a chicken homolog of the neural cell adhesion molecule L1 in consolidation of memory for a passive avoidance task in the chick. Learn. Mem 1995;2:17–25. [PubMed: 10467563]

Shoop RD, Martone ME, Yamada N, Ellisman MH, Berg DK. Neuronal acetylcholine receptors with α7 subunits are concentrated on somatic spines for synaptic signaling in embryonic chick ciliary ganglia. J. Neurosci 1999;19:692–704. [PubMed: 9880590]

Shoop RD, Esquenazi E, Yamada N, Ellisman MH, Berg DK. Ultrastructure of a somatic spine mat for nicotinic signaling in neurons. J. Neurosci 2002;22:748–756. [PubMed: 11826104]

Triana-Baltzer GB, Liu S, Berg DK. Pre- and postsynaptic actions of L1-CAM in nicotinic pathways. Mol. Cell. Neurosci 2006;33:214–226. [PubMed: 16952465]

Varoqueaux F, Aramuni G, Rawson RL, Mohrmann R, Missier M, Gottmann K, Zhang W, Sudhof TC, Brose N. Neuroligins determine synapse maturation and function. Neuron 2006;51:741–754. [PubMed: 16982420]

Williams BM, Tamburni MK, Schwartz Levey M, Bertrand S, Bertrand D, Jacob MH. The long internal loop of the α3 subunit targets nAChRs to subdomains within individual synapses on neurons in vivo. Nat. Neurosci 1998;1:557–562. [PubMed: 10196562]

Wilson Horch HL, Sargent PB. Perisynaptic surface distribution of multiple classes of nicotinic acetylcholine receptors on neurons in the chicken ciliary ganglion. J. Neurosci 1995;15:7778–7795. [PubMed: 8613719]

Zhang ZW, Vijayaraghavan S, Berg DK. Neuronal acetylcholine receptors that bind α-bungarotoxin with high affinity function as ligand-gated ion channels. Neuron 1994;12:167–177. [PubMed: 7507338]

NIH-PA Author Manuscript
NIH-PA Author Manuscript
NIH-PA Author Manuscript

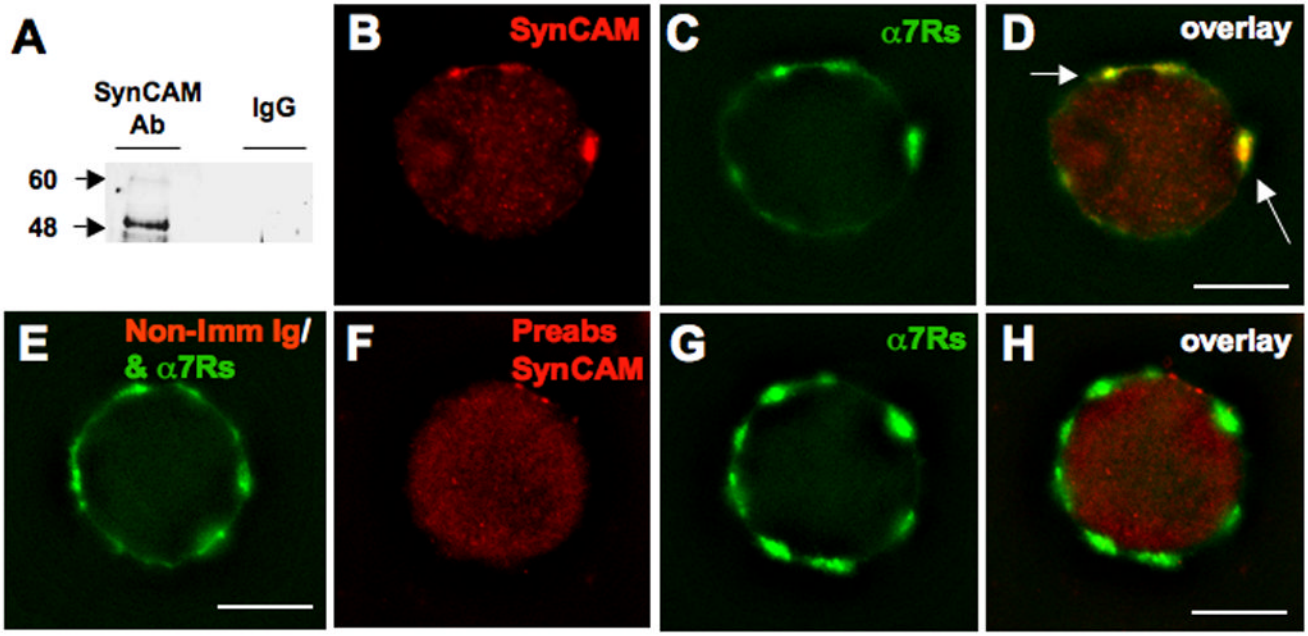

Figure 1.

SynCAM is expressed in CG neurons and co-localizes with nAChRs. E14 CG lysate was subjected to SDS-PAGE and Western Blot and then probed with either an anti-SynCAM antibody or non-immune rabbit Ig to assay for SynCAM protein expression. **(A)** Specific bands at approximately 48 and 60 kDa represent core and heavily glycosylated SynCAM, respectively. Freshly dissociated E14 CG neurons were **(B)** immunostained for SynCAM (red), and **(C)** costained with αBgt for α7-nAChRs (green), and **(D)** the images merged to display overlaid clusters (yellow, arrows). **(E)** Substituting non-immune rabbit Ig for SynCAM, as a negative control, revealed the absence of the large SynCAM clusters, suggesting these clusters represent specific staining. **(F)** Preabsorption of the SynCAM antibody with a peptide corresponding to the SynCAM cytoplasmic domain abolished the large SynCAM clusters (red), but **(G)** did not affect staining for α7-nAChRs (green), also shown **(H)** with the images merged to display overlay, again confirming the specificity of the anti-SynCAM antibody. Number of experiments: 2 in A; 3 in B–H. Scale bars: 10 μM.

NIH-PA Author Manuscript
NIH-PA Author Manuscript
NIH-PA Author Manuscript

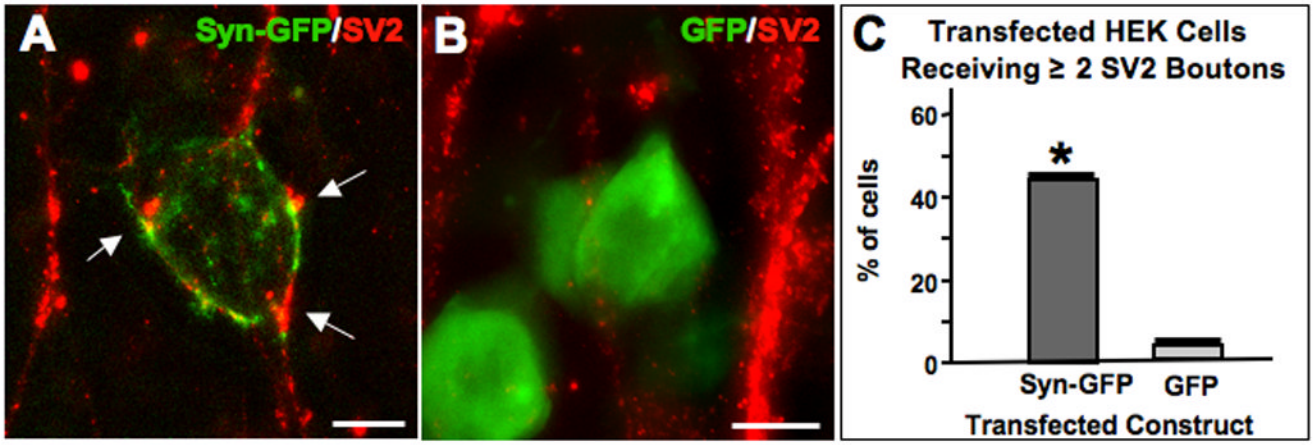

Figure 2.

Heterologously expressed SynCAM induces presynaptic specializations in adjacent cholinergic neurons. HEK293 cells were transfected with constructs encoding **(A)** SynCAM-GFP (green), or **(B)** GFP (green) and grown for 2 days with E8 CG neurons that had been in culture for 4 days; cells were immunostained for SV2 (red) and imaged. **(C)** Quantifying the proportion of transfected HEK cells per culture contacted by multiple SV2 clusters showed that SynCAM-GFP significantly increased the amount of SV2 clusters abutting the transfected HEK cells (arrows in A) while GFP did not. Values represent the mean ± SEM of 3–4 separate experiments. *$p < 0.05$ compared to GFP using Student's t-test. Scale bars: 10 μm.

NIH-PA Author Manuscript
NIH-PA Author Manuscript
NIH-PA Author Manuscript

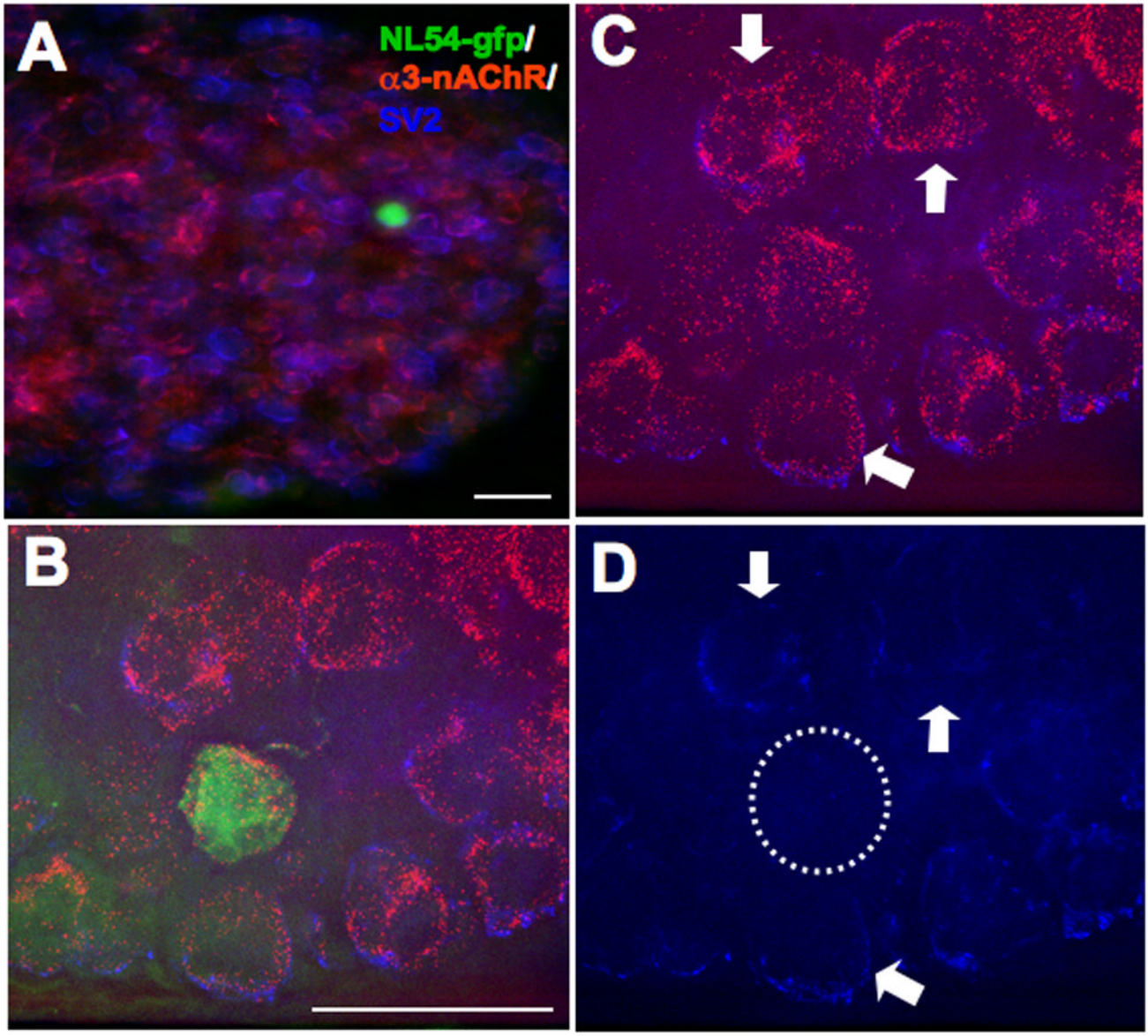

Figure 3.

Electroporation of early embryo introduces constructs into isolated neurons in the developing CG in vivo. E2 chick embryos were electroporated with GFP-tagged L1, NL, or SynCAM dominant negatives and then allowed to incubate. At E14 the CGs were dissected from these embryos and coimmunostained for α3*-nAChRs (red) and SV2 (blue), followed by imaging to visualize both along with GFP expression (green) as a marker for transfected cells **(A)**. Analysis of relative nAChR and SV2 levels was performed on higher magnification images **(B)** after first deleting the fluorescence signal from unneeded channels, i.e. visualizing solely the nAChR and SV2 staining **(C)**, or the SV2 staining alone **(D)**. NL54-GFP transfected neurons (dashed circle) exhibit far fewer SV2 puncta overlaying the soma than do control neurons in the vicinity (arrows); they have normal α3*-nAChR patterns **(D)**. Scale bars: 40 μm.

NIH-PA Author Manuscript
NIH-PA Author Manuscript
NIH-PA Author Manuscript

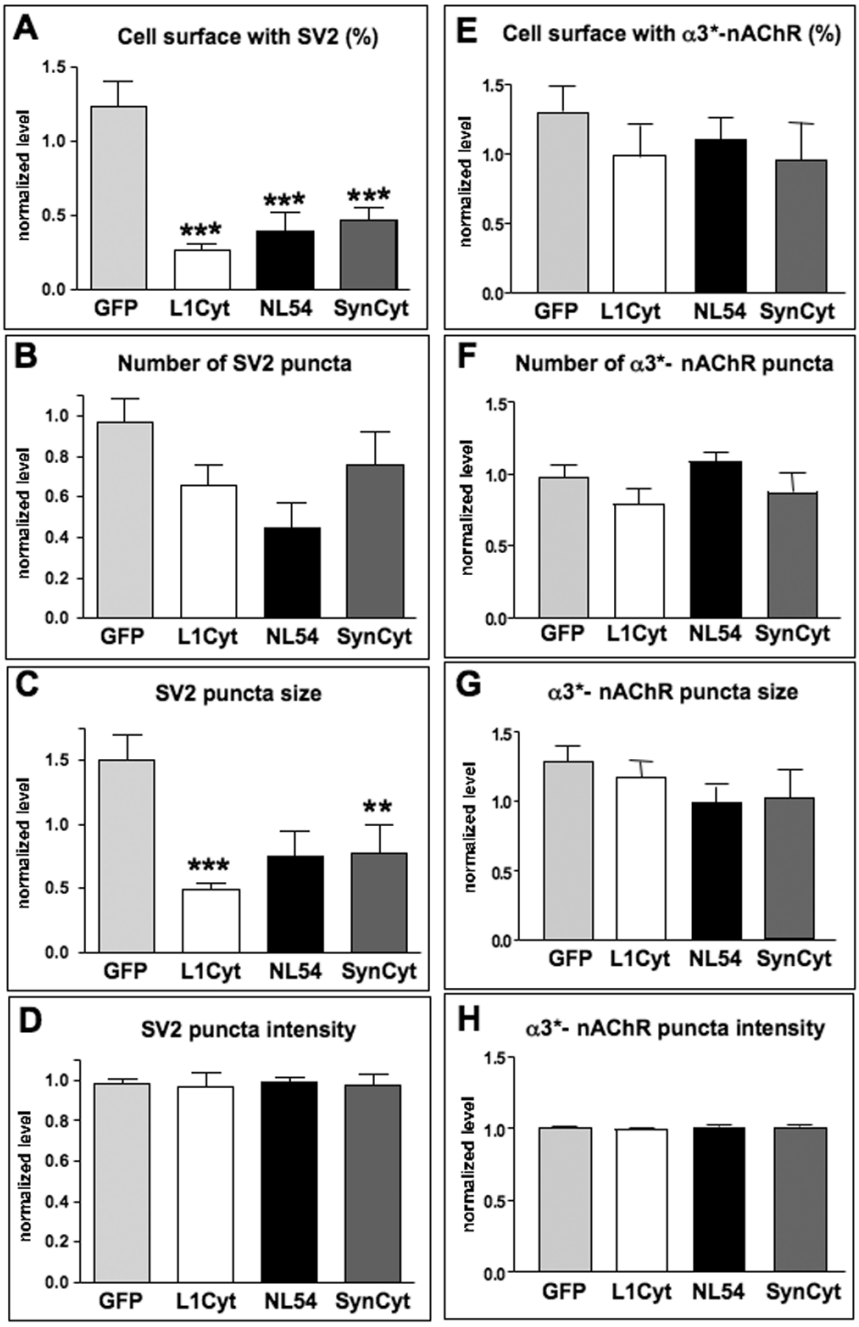

Figure 4.

L1, neuroligin, and SynCAM are each necessary for maintaining proper SV2 levels abutting transfected neurons but do not affect nAChR levels or patterns on transfected neurons. Electroporated E14 CG neurons were coimmunostained for SV2 and α3*-nAChRs; specific staining levels were quantified from deconvolved fluorescence images. Values for transfected cells were normalized to the average found for several untransfected adjacent cells. **(A)** Quantification revealed significant reductions in the levels of SV2 abutting neurons transfected with L1Cyt-GFP, NL54-GFP, or SynCyt-GFP, in contrast to neurons transfected with GFP as a negative control. Quantifying the number of SV2 puncta yielded nominal decrements for all three constructs **(B)**, whereas significant decrements were caused by L1Cyt-GFP and by

NIH-PA Author Manuscript

NIH-PA Author Manuscript

NIH-PA Author Manuscript

SynCyt-GFP in the mean size of the puncta overlaying the soma **(C)**. The mean intensity of SV2 puncta contacting the soma **(D)** was not altered by any of the constructs. Quantifying α3*-nAChR staining for the same four parameters (**E–H**) revealed no significant change induced by any of the transfected constructs. *$p < 0.05$; **$p < 0.01$; ***$p < 0.001$ compared to GFP by ANOVA with Bonferroni post-tests. Number of electroporated cells analyzed for SV2 was 44, 43, 12, and 39 for GFP, L1Cyt, NL54, and SynCyt, respectively (1–4 cells per ganglion), and for α3*-nAChR clusters it was 22, 12, 10, and 15, respectively, together with 2–4 nearby unelectroporated control cells in the same section for each electroporated cell.

NIH-PA Author Manuscript
NIH-PA Author Manuscript
NIH-PA Author Manuscript

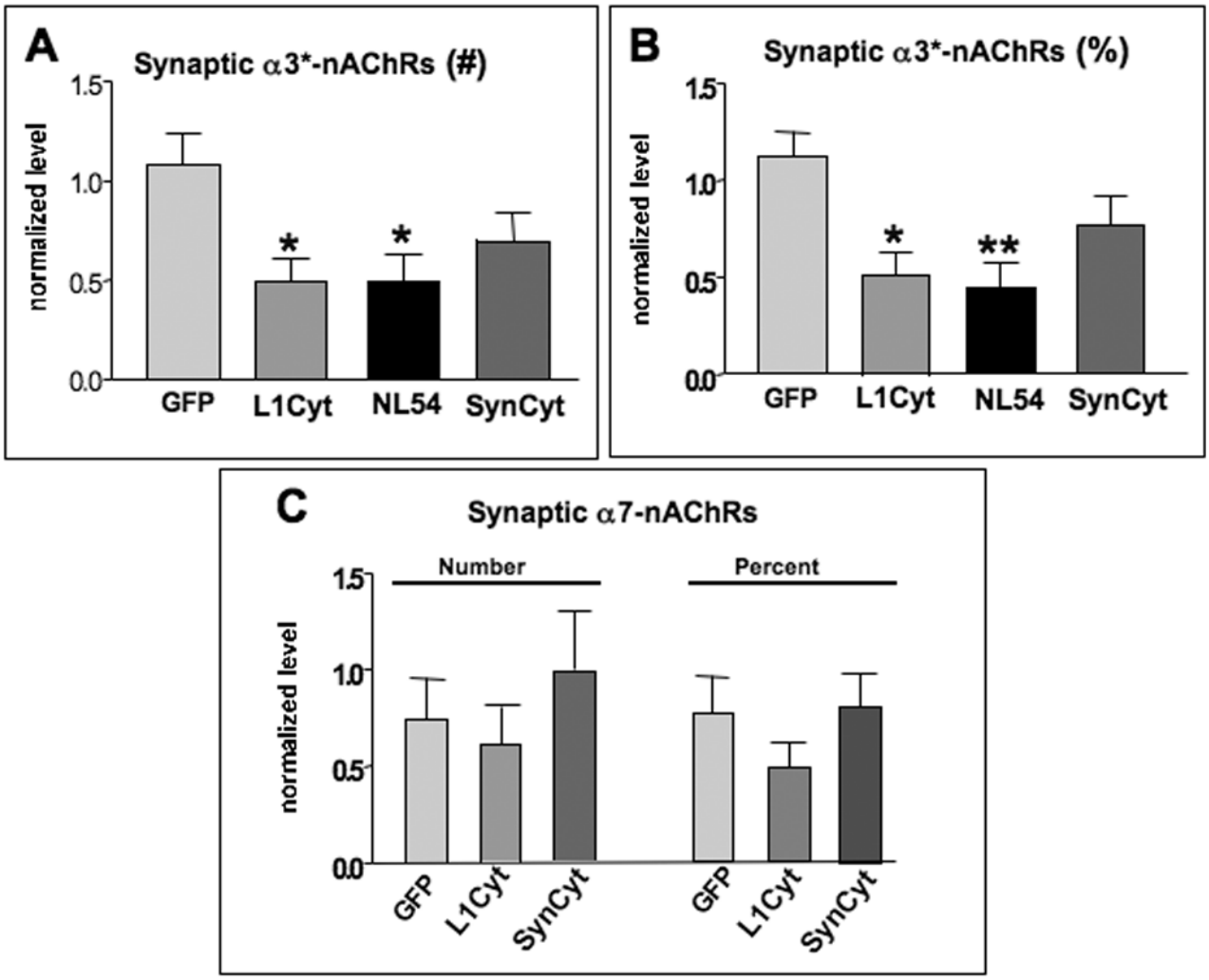

Figure 5.

L1 and NL are each necessary for maintaining innervation of synaptic α3*-nAChRs on transfected neurons. Electroporated E14 CG neurons were coimmunostained for SV2 and α3*-nAChRs, followed by quantitative image analysis as in Fig. 4. Neurons transfected with L1Cyt or NL54 had significantly lower total numbers of α3*-nAChR clusters overlaid by SV2 puncta **(A)**, apparent also as a reduced fraction of α3*-nAChR clusters overlaid by SV2 puncta **(B)**. SynCyt did not significantly reduce either. Neither SynCyt nor LiCyt changed either the total number or the proportion of α7-nAChR clusters overlaid by SV2 puncta **(C)**. *$p < 0.05$; **$p < 0.01$ compared to GFP by ANOVA with Bonferroni post-tests. Number of cells analyzed were as in Fig. 4 for panels A and B; for panel C, the number was 8, 27, and 24 for GFP, L1Cyt, and SynCyt, respectively (1–4 cells per ganglion), plus 2–4 unelectroporated control cells in the same section for each electroporated cell.

NIH-PA Author Manuscript
NIH-PA Author Manuscript
NIH-PA Author Manuscript

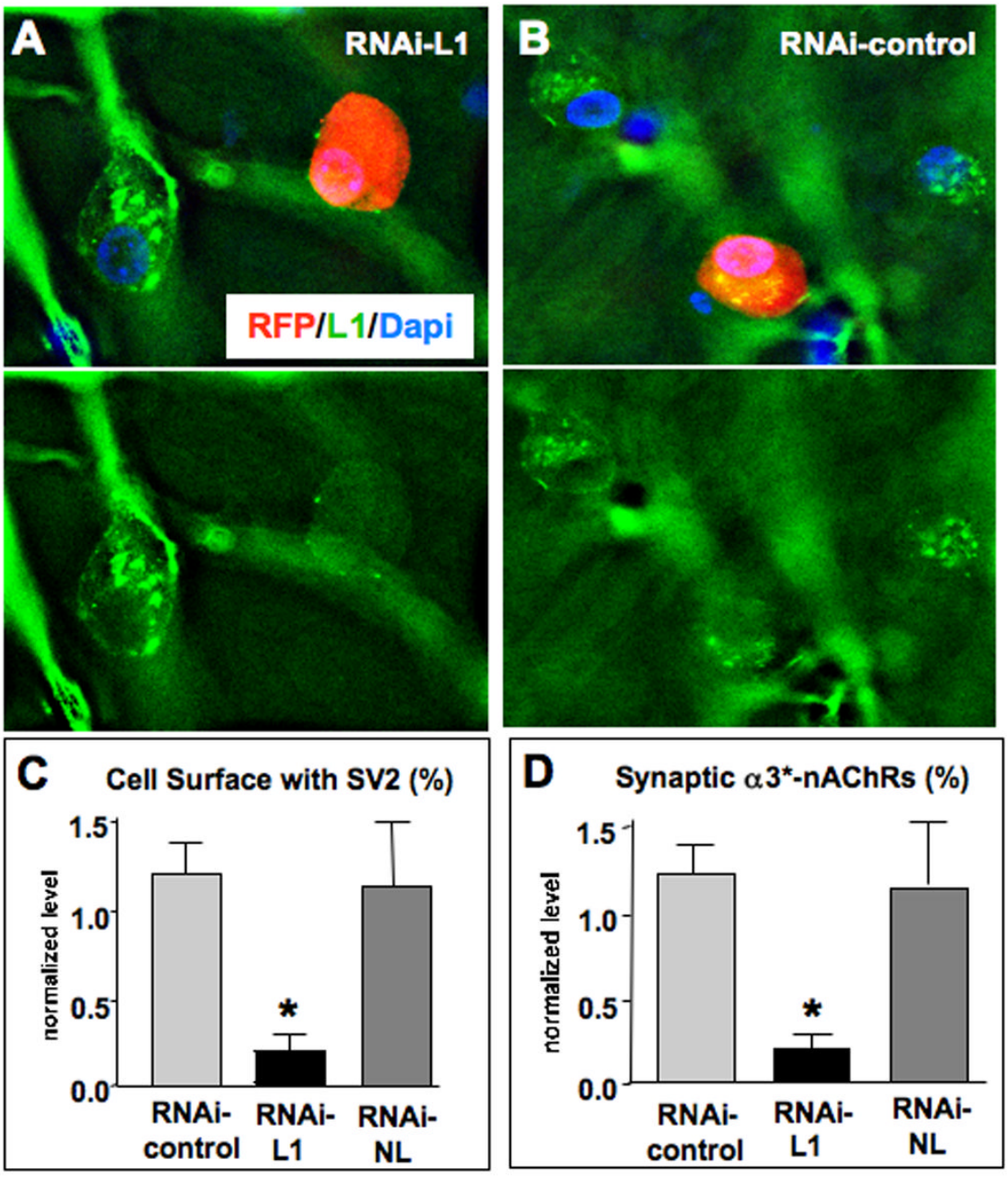

Figure 6.

L1 RNAi show reduces innervation of α3*-nAChR clusters in ovo. **(A)** CG neurons transfected in culture with a construct encoding an RNAi against chicken L1 and RFP as a marker (red) showed lower levels of endogenous L1 as seen by immunostaining (green) than did nearby untransfected cells. This is most evident when viewing the images with the RFP fluorescence deleted to reveal the L1 stain (bottom). **(B)** An RNAi with a scrambled sequence (RNAi-control) had no effect on L1 levels. **(C)** Electroporation of CG neurons in ovo revealed significant reductions in SV2 levels abutting RNAi-L1 transfected cells compared to RNAi-control transfected cells, similar to the pattern seen with the L1Cyt-GFP construct. In contrast transfection with an RNAi construct that targets neuroligin (RNAi-NL) had no affect on SV2

NIH-PA Author Manuscript

NIH-PA Author Manuscript

NIH-PA Author Manuscript

levels. **(D)** Quantifying the proportion of α3*-nAChR clusters with SV2 clusters apposed, to assay for potential synapses, revealed a similar pattern. Cells transfected with RNAi-L1, but not with RNAi-NL, had a significantly reduced fraction of α3*-nAChR clusters receiving SV2 puncta. *$p < 0.05$ compared to RNAi-control by ANOVA with Bonferroni post-tests; 8, 6, and 10 cells examined for Control, L1, and NL RNAi's, respectively (1–4 cells per ganglion), plus 2–4 unelectroporated control cells per electroporated cell in the same section. Scale bars: 10 μm.

NIH-PA Author Manuscript
NIH-PA Author Manuscript
NIH-PA Author Manuscript

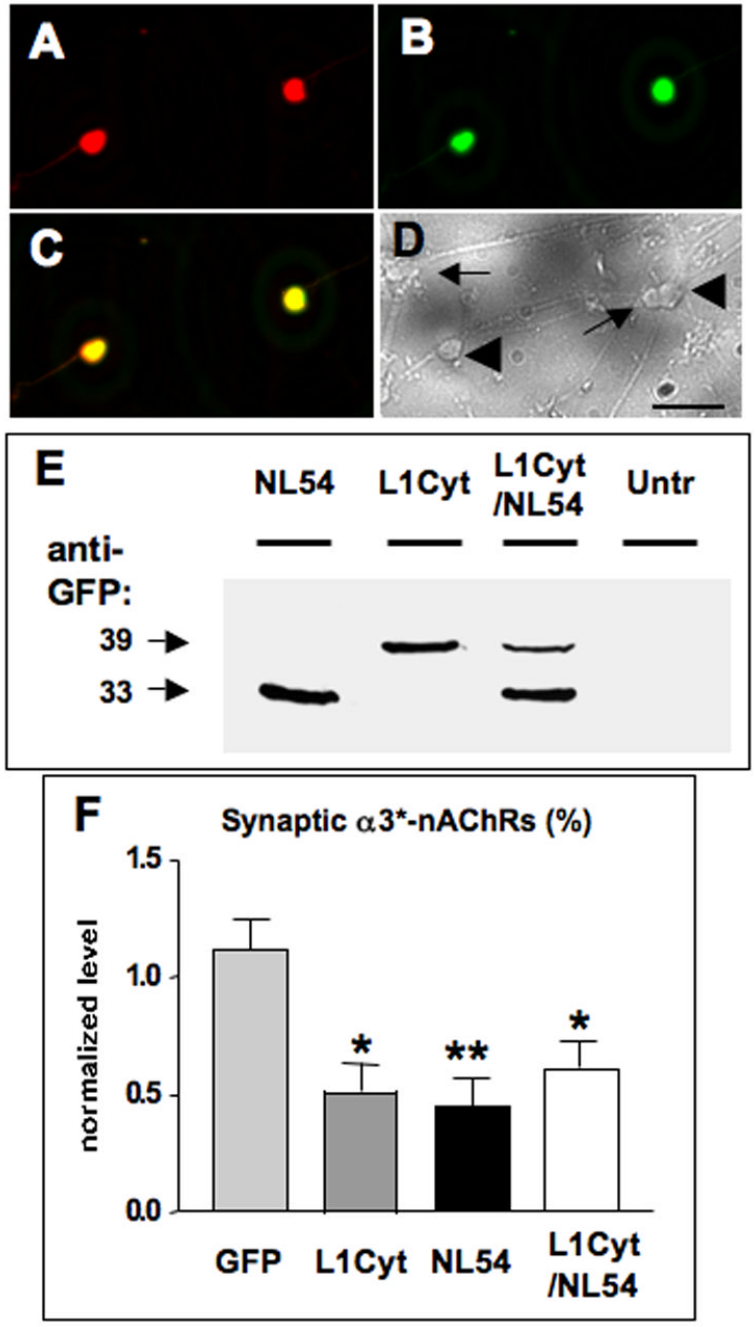

Figure 7.

Simultaneous L1 and NL disruption indicates that both are necessary for the same population of synapses. CG neurons in culture were transfected with a construct encoding both L1Cyt-GFP and NL54-GFP (L1Cyt/NL54) and then immunostained with a specific anti-human L1 antibody to discriminate between L1Cyt and endogenous chicken L1. The L1 antibody recognized **(A)** the L1Cyt peptide (red) in each **(B)** GFP-expressing cell (green), seen **(C)** in the overlay (yellow), but not **(D)** in any untransfected cells as seen in a brightfield image from the same field of view (untransfected cells, arrows; transfected cells, large arrowheads). **(E)** Western blots of culture lysates probed for GFP to reveal NL54-GFP and L1Cyt-GFP (33 and 39 kDa, respectively), confirming that both are expressed from the L1Cyt/NL54 construct.

NIH-PA Author Manuscript

NIH-PA Author Manuscript

NIH-PA Author Manuscript

Untransfected cultures showed no bands (Untr), confirming specificity. Similar results were obtained in a second experiment. Electroporation of CG neurons in ovo followed by image analysis indicated that expression of L1Cyt, NL54, or L1Cyt/NL54 each significantly reduced the proportion of α3*-nAChR clusters overlaid with SV2 puncta. **(F)** The reduction caused by L1Cyt/NL54 is quantitatively indistinguishable from similar reductions produced by either L1Cyt or NL54 alone (from Fig 5B). *$p < 0.05$; **$p < 0.01$ compared to GFP by ANOVA with Bonferroni post-tests. Cell numbers for GFP, L1Cyt, and NL54 were as in Fig. 4; 22 cells were analyzed for the L1Cyt/NL54 construct (1–4 cells per ganglion), plus 2–4 unelectroporated control cells for each electroporated cell in the same section. Scale bars: 40 μm.